Volume 1 | Number 1 | Jan 2013 | Pages 1–100

Food & Function

Linking the chemistry and pyhsics of food with health and nutrition
www.rsc.org/foodfunction

ROYAL SOCIETY OF CHEMISTRY

ROYAL SOCIETY OF CHEMISTRY

www.rsc.org/foodfunction

1   **Raspberry pulp polysaccharide inhibits tumor growth via**

2   **immunopotentiation and enhances Docetaxel chemotherapy**

3   **against malignant melanoma *in vivo***

4

5   Yong-Jing Yang,[a,d] Han-Mei Xu,[b] You-Rui Suo*[a,c]

6   *[a] Northwest Institute of Plateau Biology, Chinese Academy of Sciences, No. 23, Xinning road,*

7   *810001 Xining, Qinghai, PR China. E-mail: yrsuo@nwipb.cas.cn; Tel: +86971-6143282; Fax:*

8   *+86971-6143282*

9   *[b] The Marine Pharmacy Department, China Pharmaceutical University, No. 239, Longmian road,*

10   *210009 Nanjing, Jiangsu, PR China. E-mail: 13913925346@126.com*

11   *[c] Qinghai University, Academy of Agriculture and Forestry Science, No. 251, Ningda road, 810001*

12   *Xining, Qinghai, PR China. E-mail: yrsuo@nwipb.cas.cn; Tel: +86971-6143282; Fax:*

13   *+86971-6143282*

14   *[d] University of Chinese Academy of Sciences, No. 19, Yuquan road, 100049 Beijing, PR China.*

15   *E-mail: yongjing223@163.com*

16

Abstract

18   It has been reported previously that the systemic efficacy of chemotherapeutic

19   agents is substantially restricted for some cancer types, including malignant

20   melanoma. Therefore, the development of more effective treatment modalities

21   remains a critical, albeit elusive, goal in anticancer therapy. The study presented here

22   evaluates the antitumor activity of raspberry pulp polysaccharide (RPP) against

23   malignant melanoma using a murine tumor-bearing model. Furthermore, the

24   underlying mechanism of this antitumor activity has also been investigated. The

25   results show that while RPP exhibits no direct cytotoxic effect on HT-29, MGC-803,

26   Hela, Bel-7402, L02 and B16F10 cells *in vitro*, it does demonstrate a dose-dependent

27   growth inhibition of melanoma *in vivo* with an inhibition ratio of 59.95% at a dose of

28   400 mg/kg. Besides this, the body weight and spleen index in tumor-bearing mice

29   have also been improved in RPP-treated groups. RPP is also found to induce

30   splenocyte proliferation and is able to upregulate the activity of immune-related

31   enzymes, including acid phosphatase (ACP), alkaline phosphatase (AKP), lactate

32   dehydrogenase (LDH) and superoxide dismutase (SOD) in the spleen of

33   tumor-bearing mice. The levels of tumor necrosis factor α (TNF-α), interferon γ

34 (IFN-γ) and interleukin 2 (IL-2) in the serum of tumor-bearing mice show to be

35 effectively increased upon RPP treatment. Histopathological analyses show that RPP

36 induces tumor tissue necrosis through increasing inflammatory cell infiltration and

37 causes no lesions to liver and kidney tissues. Remarkably, RPP further enhances the

38 antitumor effect of the chemotherapeutic drug Docetaxel and alleviates

39 Docetaxel-induced liver and kidney lesions in tumor-bearing mice. These findings

40 indicate that RPP exhibits antitumor activity *in vivo* against malignant melanoma,

41 partly through enhancing the cellular immune response of the host organism. In

42 summary, RPP features critical properties to potentially find use as an

43 immunopotentiating agent or as a chemotherapy adjuvant agent for the treatment of

44 malignant melanoma.

45 **Keywords** raspberry pulp polysaccharide; antitumor; immunopotentiation;

46 combination therapy

47 **1. Introduction**

48 Cancer remains one of the most common causes of death. Chemotherapy and

49 radiotherapy are the most common treatment options of cancer, used separately or in

50 combination with each other. The primary goal of cancer therapy is to achieve

51 maximal antitumor efficacy with minimal toxicity to healthy cells and tissues.

52 Unfortunately, the non-specificity and cumulative toxicity exhibited by

53 chemotherapeutic drugs may result in severe side effects, including myelosuppression,

54 mucositis, dermatitis, diarrhea etc. [1]. Malignant melanoma proves to be one of the

55 most aggressive cancer types, with increasing incidences of melanoma around the

56 globe. Even more concerning, common resistance phenomena observed for standard

57 chemotherapeutics generally limit the efficacy of systemic therapy used to treat this

58 metastatic disease [2].

59 One of the most common reasons for the rapid progression of cancer is that some

60 tumor cells are able to escape the normal immune surveillance and control of the body

61 through the secretion of immunosuppressive factors [3]. Similarly, common

62 chemotherapies also exhibit immune suppression, which proves to be a main

63   disadvantage associated with common chemotherapeutic agents used today.

64   Polysaccharides are a class of natural macromolecules featuring a variety of

65   pharmacological activities, including antitumor [4], immunomodulatory [5],

66   antioxidant [6], antimicrobial [7] and antidiabetic [8] effects. Therefore, this class of

67   compounds prove to be one of the most studied natural functional extracts in recent

68   years [9]. Among other pharmacological properties of polysaccharides,

69   immunomodulation and antitumor effects prove to be the primary act focus of such

70   biological response modifiers. For the past few years, numerous polysaccharides,

71   particularly derived from plants such as *Gynostemma pentaphyllum* [10] and *Salvia*

72   *chinensis* [11], have been demonstrated to exhibit anti-tumor and immunomodulatory

73   properties.

74   Raspberry (*Rubus idaeus* L.) is a perennial shrub belonging to the diverse *Rubus*

75   *genus* rank. The berries of *Rubus idaeus* L. are among the most popular berries in the

76   world. Raspberries are consumed as fresh fruits or processed to jams, juices, wines or

77   may served as ingredients in other products and various foods. In recent years, the

78   scientific interest in studying the biological properties of raspberries has been growing.

79   The dietary intake of raspberries has been shown to result in various beneficial effects,

80   e.g. on cardiovascular diseases, obesity, cancer and degenerative diseases [12]. The

81   effects are most likely due to the presence of a large number of bioactive substances

82   in these berries, including flavonoids, tannins, phenolic acids, stilbenoids,

83   polysaccharides, vitamins and minerals [13, 14]. Within the last few decades, the

84   majority of research involving raspberries has focused on separation, structural

85   characterization or evaluation of bioactive properties of anthocyanins, phenols, ellagic

86   acids, triterpenes or diterpenoid compounds [15-20]. However, very little information

87   is available on extraction, structural properties and biological activities of

88   polysaccharides from raspberries.

89   According to our previous studies, raspberries prove to exhibit a very high

90   polysaccharide content (the yield of polysaccharide in the pulp of raspberry cultivated

91   in Qinghai plateau is up to 12%). Therefore, raspberries provide an ideal material for

92   the extraction of polysaccharide. The study presented here focuses on the therapeutic

93　effect of raspberry pulp polysaccharide (RPP) against malignant melanoma *in vivo*.

94　Furthermore, investigations on the possible mechanisms involved in this biological

95　activity are being discussed. In addition, the effectiveness of combining RPP and the

96　known chemotherapeutic drug Docetaxel has also been studied.

97　2.　**Materials and Methods**

98　*2.1. Materials and chemicals*

99　　Raspberries (cultivar: Heritage) have been obtained in October 2013 from Qinghai

100　Yaochi Biological Technology Co. (Huzhu, Qinghai, China). Until usage, the

101　collected sample was dried and stored at room temperature. Dulbecco's Modified

102　Eagle Media (DMEM), Roswell Park Memorial Institute-1640 (RPMI-1640) culture

103　medium and fetal bovine serum (FBS) have been purchased from Shanghai Sangon

104　Biological　Engineering　Technology　&　Services　Co.　(Shanghai,　China).

105　3-(4,5-Dimethythiazol-2-yl)-2,5-diphenyltetrazolium bromide (MTT), concanavalin A

106　(Con A) and dextran standards were all purchased from Sigma-Aldrich Co. (St. Louis,

107　MO, USA). Reagent kits for alkaline phosphatase (AKP), acid phosphatase (ACP),

108　superoxide　dismutase　(SOD),　lactate　dehydrogenase　(LDH),　BCA　protein

109　quantification and enzyme-linked immune-sorbent assay (ELISA) kits for mouse

110　tumor necrosis factor α (TNF-α), mouse interferon γ (IFN-γ), mouse interleukin 2

111　(IL-2) were all purchased from Nanjing Jiancheng Bioengineering Institute (Nanjing,

112　Jiangsu, China).

113　*2.2. Cell lines*

114　　B16F10 mouse melanoma cells were provided by The Key Laboratory of Modern

115　Chinese Medicines of China Pharmaceutical University. Cell lines of human hepatic

116　carcinoma Bel-7402, human cervical carcinoma Hela, human colon carcinoma HT-29,

117　human gastric carcinoma MGC-803 and human normal hepatocyte L02 have all been

118　obtained from the American type Cell Culture (ATCC, Shanghai, China).

119　*2.3. Preparation of polysaccharide from raspberry pulp*

120　　The powder, produced after drying and grinding the pulp, was sieved in order to

121　remove　any　seeds　present　and　was　then　double-extracted　with　petroleum　ether

4

122   (boiling point, 60-90˚C) at room temperature for 24 hours upon continuous stirring.

123   The defatted sample was then extracted with 80% ethanol at 60˚C for 2 hours to

124   remove any colored contaminants, monosaccharides, oligosaccharides and other small

125   molecules. The residue was suspended in distilled water and the extraction of

126   polysaccharide was carried out via ultrasound at 60˚C for 2 hours. The filtrate was

127   subsequently combined and concentrated in vacuo using a flash evaporator at 60˚C.

128   The concentrated portion was deproteinated according to the Sevage method [21], for

129   a total of three times. Thereafter, a 4-fold volume of 95% ethanol was added to

130   precipitate the polysaccharide at 4˚C overnight. The precipitate was collected by

131   centrifugation (3000 × g, 10 min) and lyophilized. The total polysaccharide content

132   was determined with the phenol-sulfuric acid method using D-glucose as a standard

133   [22]. Contaminant endotoxin was analyzed with a limulus amebocyte lysate (LAL)

134   assay [23].

135   *2.4. Primary structural analysis of RPP*

136   *2.4.1. FTIR spectroscopic analysis*

137   The IR spectrum of RPP was carried out using a Fourier transform infrared

138   spectrophotometer. The sample was ground with spectroscopic grade potassium

139   bromide (KBr) powder and was then pressed into 1 mm pellets for FT-IR analysis in

140   the frequency range of 400 to 4000 cm^{-1}.

141   *2.4.2. SEM microstructural analysis*

142   The polysaccharide was coated with a thin layer of gold under reduced pressure

143   and was then examined using a SEM system (JSM-7500, JEOL, Japan) at 5 kV

144   acceleration voltage and image magnifications of 10000×, 5000× 2000×and 1000×.

145   *2.4.3. Analysis of monosaccharide composition of RPP*

146   The   analysis   of   the   monosaccharide   was   performed   by   the   gas

147   chromatography-mass spectrometry (GC-MS) method. Briefly, RPP (5 mg) was

148   dissolved in 4 ml of a 2 mol/L trifluoroacetic acid (TFA) solution in a sealed glass

149   tube and was subsequently hydrolyzed at 110˚C for 4 hours. After removal of residual

150   TFA by co-concentrating repeatedly with methanol at 50˚C, the sample was dissolved

151   in 0.1 ml of pyridine and reacted with 5 mg of hydroxylamine hydrochloride for 30

5

152 min at 90°C. Next, 0.1 ml of acetic anhydride was added to the mixture and

153 incubation was continued for another 3 hours at 90°C. Finally, the sample was dried

154 and dissolved in 800 μl of chloroform. Seven monosaccharide standards, including

155 rhamnose, arabinose, fructose, xylose, galactose, mannose, glucose and lactose were

156 converted to their acetylated derivatives according to the method described above.

157 The samples were injected into a gas chromatograph (7890A, Agilent Technology)

158 instrument equipped with a hydrogen flame ionization detector (FID) using a

159 DB-5MS UI capillary column (30m×0.25mm×0.25μm). The following

160 chromatographic conditions were used: high-purity helium was used as the carrier gas

161 at a flow rate of 1 ml/min. The temperature of the injector and detector was 250°C.

162 The initial column temperature was set to 100°C followed by 5°C/min increases. As

163 the temperature reaches 200°C, it was maintained for 1 min and then increased to

164 250°C in 10°C/min increments. Injections were performed in a splitless mode. The

165 temperature of the mass spectrometer ion source was 280°C.

166 *2.4.4. Molecular weight distribution of RPP*

167 The molecular weight distribution of RPP was determined using gel-permeation

168 chromatography (GPC) on a LC-20AT instrument (Shimadzu, Tokyo, Japan),

169 equipped with a SB-802 column in series with a SB-805 column (Showa, Takasaki,

170 Japan). A solution of 0.1 mol/L sodium nitrate ($NaNO_3$) was used as the eluent at a

171 flow rate of 0.4 ml/min. The temperature was set at 30°C. The individual peaks were

172 detected using a refractive index detector (Shimadzu, RID-10A). Dextran

173 (Sigma-Aldrich, St. Louis, MO. USA) with molecular weight of 805000, 393000,

174 210000, 48800, 21700, 10000, 6000 and 180 Da were used as molecular weight

175 standards.

176 *2.5. In vitro cytotoxicity assay*

177 Cell lines including Bel-7402, B16F10, Hela, HT-29, MGC-803 and L02 were

178 used to evaluate the cytotoxicity of RPP *in vitro*. The cells were washed with PBS and

179 dispersed in a 0.05% trypsin solution. After centrifugation, the cell pellets were

180 resuspended in a DMEM medium (10% FBS) at a density of 2×10^4 cells/ml,

181 subsequently seeded in a 96-well plate (2×10^3 cells/well) and incubated overnight.

182 The cells were treated with 10 μg/ml Docetaxel (as a positive control) and a series of

183 doses of RPP (1, 2, 4, 8, 16, 32, 64, 128 and 256 μg/ml). Neat DMEM medium was

184 used as a blank control. Each concentration was repeated 5 times. After incubation for

185 48 hours, 20 μl of MTT (5 mg/ml) was added to each well. After incubation for

186 another 4 hours, the supernatant was decanted off and 150 μl of DMSO was added to

187 dissolve the formazan precipitate. The optical density was then measured at 570 nm

188 using a microplate reader. The assays have been independently repeated for a total of

189 three times.

190 *2.6. In vivo acute toxicity assay*

191   In an effort to evaluate the toxicity of RPP on the biological systems, an acute

192 toxicological test has been performed. Kunming mice (6-8 weeks old, 18-22 g) have

193 been obtained from the Qinglong Experimental Animal Center of Nanjing (Jiangsu,

194 China). The mice, half males and half females, were assigned randomly into three

195 individual groups with 10 mice in each group. RPP was dissolved in phosphate

196 buffered saline (PBS). After fasting the mice overnight, RPP was administered to each

197 group intragastrically, at dose of 100 mg/kg, 500 mg/kg and 2000 mg/kg, respectively.

198 The mice were closely monitored for any obvious changes in vitality in 4 hour

199 intervals. The mortality ratio within 72 hour time period was recorded and the

200 individual dose required to kill 50% of the mouse population (i.e. LD_{50}) was assessed.

201 We hereby assure that all experiments involving animals have been carried out

202 according to the ethical standards set by the University of Chinese Academy of

203 Sciences. The care and maintenance of the animals was in accordance with the

204 licensing guidelines of the University of Chinese Academy of Sciences. The

205 institutional committee has approved the protocol used for the animal experiments.

206 *2.7. In vivo antitumor assay*

207 *2.7.1. Animals*

208   Female C57BL/6 mice (6-8 weeks old, 18-22 g) were purchased from the

209 Qinglong Experimental Animal Center of Nanjing (Jiangsu, China). We hereby assure

210 that all experiments involving animals have been carried out according to the ethical

211 standards set by the University of Chinese Academy of Sciences. The care and

212   maintenance of the animals was in accordance with the licensing guidelines of the

213   University of Chinese Academy of Sciences. The institutional committee has

214   approved the protocol used for the animal experiments.

215   *2.7.2. Tumor implantation*

216   B16F10 mouse melanoma cells were maintained in DMEM culture medium

217   supplemented with 10% FBS, 100 IU/ml penicillin and 100 μg/ml streptomycin in a

218   humidified atmosphere at 37˚C with 5% carbon dioxide (CO_2). The cells were washed

219   with phosphate buffered saline (PBS) and dispersed in a 0.05% trypsin solution. After

220   centrifugation at 2000 × g for 5 minutes, the cell pellets were resuspended in PBS and

221   adjusted to a concentration of 5×10^6 cells/ml. 5×10^5 B16F10 cells were implanted

222   into each mouse on the mid-right side subcutaneously (s.c.).

223   *2.7.3. C57BL/6 mice treatment*

224   After the average tumor volume of melanoma had reached 60 mm^3, mice were

225   randomly divided into 5 groups. The model control (MC) received PBS. The positive

226   control (PC) was injected subcutaneously with Docetaxel (purchased from Hengrui

227   Pharmaceutical Co., Jiangsu, China) once every three days at a dose of 10 mg/kg. The

228   low dose group (LDG), the medium dose group (MDG) and the high dose group

229   (HDG) were fed with RPP by oral gavage once daily at dose of 100, 200, and 400

230   mg/kg, respectively.

231   After treating the mice for 2 weeks, the animals were anesthetized and the body

232   weight was assessed. Blood samples were collected from the eyes. The blood serum

233   was obtained by centrifuging the blood samples for 10 minutes at 2500 × g at 4˚C.

234   The mice were then sacrificed by cervical dislocation and the tumor tissues were

235   extracted from the animals, weighted, photographed and fixed with 10%

236   formaldehyde for subsequent histopathology studies. The spleen was removed and the

237   weight was recorded before homogenization. The liver and kidneys were obtained and

238   fixed with 10% formaldehyde for histopathology studies. The liver and kidney tissues

239   from several other healthy female C57BL/6 mice were used as normal control in the

240   histopathology analyses.

241   *2.7.4. Measurement of tumor growth*

242   The tumor sizes were measured individually using a vernier caliper once every

243   other day. The tumor volume was calculated according to the following formula:

244   tumor volume = length $\times$ width^2 $\times$ 0.52. The therapeutic effects on the tumor growth

245   have been expressed as the mean tumor volume versus time, calculated as (1-T/C)

246    $\times$100%, where T describes the treated tumor volume and C determines the model

247   control tumor volume.

248   *2.8. Histopathology observation*

249   The tissues, fixed with 10% formaldehyde, were embedded in paraffin and

250   sectioned for hematoxylin and eosin (H&E) staining. The sections have been observed

251   and photographed at 100× and 400×magnifications.

252   *2.9. Ex vivo splenocyte proliferation assay*

253   The spleens were quickly and aseptically removed from the sacrificed mice. They

254   were gently homogenized and passed through a 40 μm nylon cell strainer in order to

255   obtain a single-cell suspension. After removing the erythrocytes, the splenocytes were

256   washed and resuspended in a RPMI-1640 medium (2% FBS) at a concentration of 1 $\times$

257   10^7 cells/ml. The cells were seeded in a 96-well plate and treated with 10 μg/ml

258   Docetaxel as well as a series of different concentrations of RPP (32, 64, 128 and 256

259   μg/ml). ConA (5 μg/ml) was used as a positive control, and neat RPMI-1640 medium

260   was used as a blank control. Each concentration was repeated for a total of 5 times.

261   After incubation at 37°C in a humidified 5% CO_2 incubator for 72 hours, 20 μl of

262   MTT (5 mg/ml) was added to each well. After incubation for another 4 hours, the

263   supernatant was removed and 150 μl of DMSO was added to dissolve the formazan

264   precipitate. The optical density was then measured at 570 nm using a microplate

265   reader. The assays were individually repeated three times.

266   *2.10. Evaluation of the activity of immune-related enzymes in the spleen*

267   Spleen homogenate was prepared using an ultrasonic cell disruptor (400 ampere, 5

268   seconds once, repeat 3times) in an ice-cold medium (pH 7.4, 0.01 mol/L Tris-HCl,

269   0.0001 mol/L EDTA-2Na, 0.01 mol/L Sucrose, 0.8% NaCl). After centrifugation for

270   10 minutes at 5000 $\times$ g at 4°C, the supernatants were used to measure the

271   immune-related enzymes activity of AKP, ACP, SOD and LDH using assay kits. The

272   optical density of AKP, ACP, SOD and LDH was found to be 520 nm, 520 nm, 550

273   nm and 440 nm, respectively. The protein content of the supernatants was quantified

274   using a BCA protein quantification kit.

275   *2.11. Assessment of TNF-α, IFN-γ and IL-2 levels in serum by ELISA*

276   The levels of TNF-α, IFN-γ and IL-2 in serum were assessed using ELISA kits

277   according to the manufacturer's instructions.

278   *2.12. Combinatory RPP-Docetaxel treatment on malignant melanoma-bearing mice*

279   Animal protocols, cell line and tumor implantation procedures have all been

280   carried out similarly to what has been described in subsections 2.7.1 and 2.7.2. The

281   mice were randomly divided into 3 groups, including the model control (MC),

282   Docetaxel group and combinatory RPP-Docetaxel group (R-D) with an average tumor

283   volume of B16F10 mouse melanoma equalling 60 mm^3. The model control received

284   PBS and the Docetaxel group has been injected with Docetaxel (purchased from

285   Hengrui Pharmaceutical Co., Jiangsu, China) subcutaneously at a dose of 10 mg/kg

286   once every three days. The combinatory RPP-Docetaxel group received Docetaxel via

287   subcutaneous injection once every three days at a dose of 10mg/kg together with RPP

288   once daily via oral gavage at a dose of 400mg/kg. The measurement of the tumor

289   growth was similar to the protocol described in subsection 2.7.4. After treatment for 2

290   weeks, the mice were sacrificed by cervical dislocation, the tumor tissues, liver,

291   kidneys were collected and the net body weight was recorded. The histopathology

292   studies of the tumor tissues, liver and kidney have been carried out similar to what has

293   been described in subsection 2.8.

294   *2.13. Statistical analysis*

295   The data were expressed as mean values ± S.E. and analyzed by one-way ANOVA

296   followed by Tukey's post hoc test using SPSS version 13.0 software (SPSS, Chicago,

297   IL, USA). The difference was considered significant if *P<0.05* and highly significant

298   if *P<0.01*.

299   **3. Results**

300   *3.1. The primary structural analysis of RPP*

301   The total polysaccharide content was found to be 91.2% ± 4.51%. RPP was

302   composed of rhamnose, arabinose, xylose, mannose, glucose and lactose, with a molar

303   ratio of 2.0:19.9:1.0:1.1:7.1:2.3. Additionally, the polysaccharide solution was found

304   to be free of endotoxins.

305   A FTIR spectrum of RPP is shown in Figure 1. The signal in the range 1200-950

306   cm^{-1} can be ascribed to the characteristic absorption peak of polysaccharides, where

307   the position and intensity of the bands could be identified [24]. The intense peaks at

308   3449 cm^{-1} and 2948 cm^{-1} are attributed to the O-H and C-H stretching vibrations,

309   respectively. The relatively strong absorption peak at 1600 to 1650 cm^{-1} is

310   characteristic for the presence of a C=O bond [25]. The group of bands ranging from

311   1485 to 1350 cm^{-1} indicate the presence of –CH (O-CH$_2$) flexural vibrations. The

312   bands at 1000 to 1200 cm^{-1} suggest the presence of glucosyl residued in pyranose

313   form from present in RPP. Finally, the absorption band at 846.3 cm^{-1} demonstrates the

314   presence of α-linked residues in RPP. The bands in the range of 350 to 600 cm^{-1} can

315   be assigned to skeletal modes of pyranose rings [26].
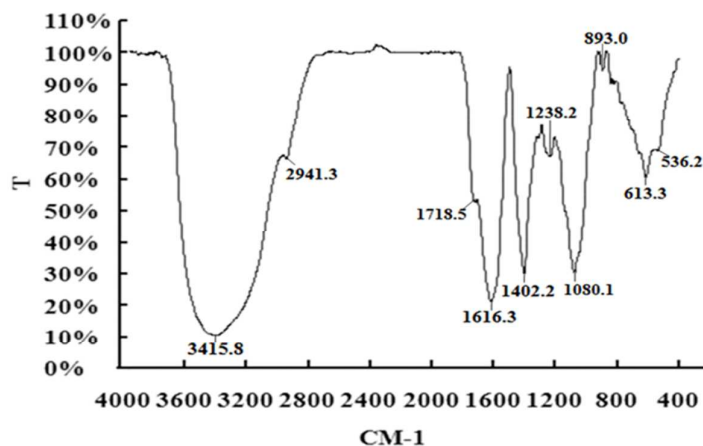
316

317   **Figure 1.** FT-IR spectra of RPP ranging from 400 to 4000 cm^{-1}.

318   As shown in Figure 2, RPP elutes as two peaks in the GPC with an average

319   molecular weight estimated to be 49926 Da (Peak 1, 32.13%) and 1823 Da (Peak 2,

320   67.87%), respectively. The molecular weight has been determined in reference to the

321   calibration curve of dextran standards.
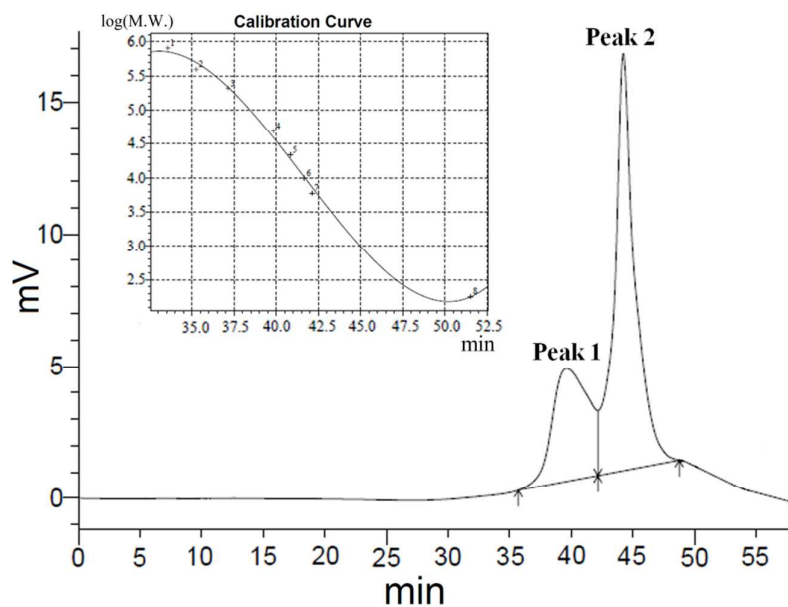
Figure 2. Molecular weight distribution of RPP.

The SEM images of RPP are shown in Figure 3. The result obtained indicates that RPP exhibits a rough surface with randomly distributed ovoid-shaped particles.
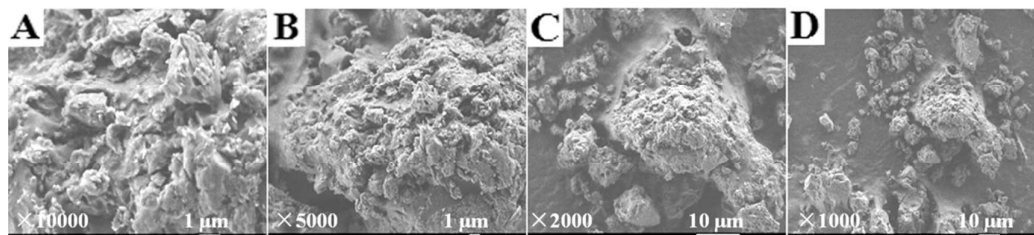
Figure 3. SEM images of RPP. A: morphology of RPP at 10000× (scalebar 1 μm). B: morphology of RPP at 5000× (scalebar 1 μm). C: morphology of RPP at 2000× (scalebar 10 μm). D: morphology of RPP at 1000× (scalebar 10 μm).

3.2. Evaluation of the in vitro cytotoxicity of RPP

The MTT method was applied in an effort to determine the cytotoxicity of RPP *in vitro*. As shown in Figure 4, RPP exhibits no obvious inhibitory effect on the proliferation of human colon carcinoma cell HT-29, human gastric carcinoma cell MGC-803, human cervical carcinoma cell Hela, human hepatic carcinoma cell Bel-7402, human normal hepatocyte L02 and mouse melanoma cell B16F10. However, due to the cytotoxic effect, Docetaxel significantly inhibited the proliferation of these cells compared to the blank control (*$**P<0.01$*), and the proliferation inhibition ratio of Docetaxel on HT-29, MGC-803, Hela, Bel-7402, L02 and B16F10 cells increases to 90.30%, 93.60%, 91.59%, 90.22%, 90.60% and

340   94.85%, respectively. These results indicated that RPP exhibits no direct cytotoxic

341   effect.
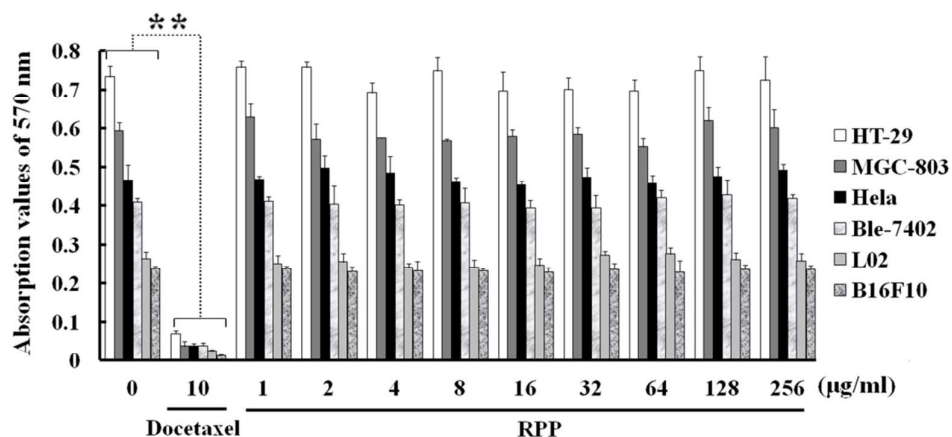
342

343   **Figure 4.** Effects of RPP and Docetaxel on proliferation of human colon carcinoma cell HT-29,

344   human gastric carcinoma cell MGC-803, human cervical carcinoma cell Hela, human hepatic

345   carcinoma cell Bel-7402, human normal hepatocyte L02 and B16F10 mouse melanoma cell. Data

346   is expressed as the mean values ± S.E. (n=5). Differences were considered to be statistically

347   significant when *P<0.05*. High significance was determined when *P<0.01*. Notes: **P<0.01 vs.*

348   blank control.

349   *3.3. Evaluation of the in vivo toxicity of RPP*

350   During the process of the acute toxicity assay *in vivo*, no behavioral changes or

351   visible toxicity symptom have been observed upon intragastrical administration of

352   RPP up to a concentration of 2000 mg/kg. Hence, the LD_{50} of RPP was determined to

353   be far more than 2000 mg/kg indicating that RPP is likely non-toxic and therefore

354   considered safe.

355   *3.4. The antitumor effect of RPP against melanoma in vivo*

356   As shown in Figure 5, RPP inhibits the growth of melanoma in a dose-dependent

357   fashion and the tumor volume inhibition ratio of low, medium and high dose RPP was

358   found to be 7.56%, 24.32% and 59.95%, respectively. The tumor volume of the high

359   dose RPP group exhibits a statistical difference compared to that of the model control

360   group (*P<0.05*). The chemotherapeutic agent Docetaxel, used as a positive control in

361   this study, has been widely clinically as a broad-spectrum antitumor drug. Our results

362   obtained show that Docetaxel can significantly inhibit the growth of melanoma

363   (***P<0.01 vs.* model control), with an inhibition ratio of tumor volume found to be

364   66.49%. However, deaths of tumor-bearing mice have been observed during

13

365   Docetaxel treatment.

366
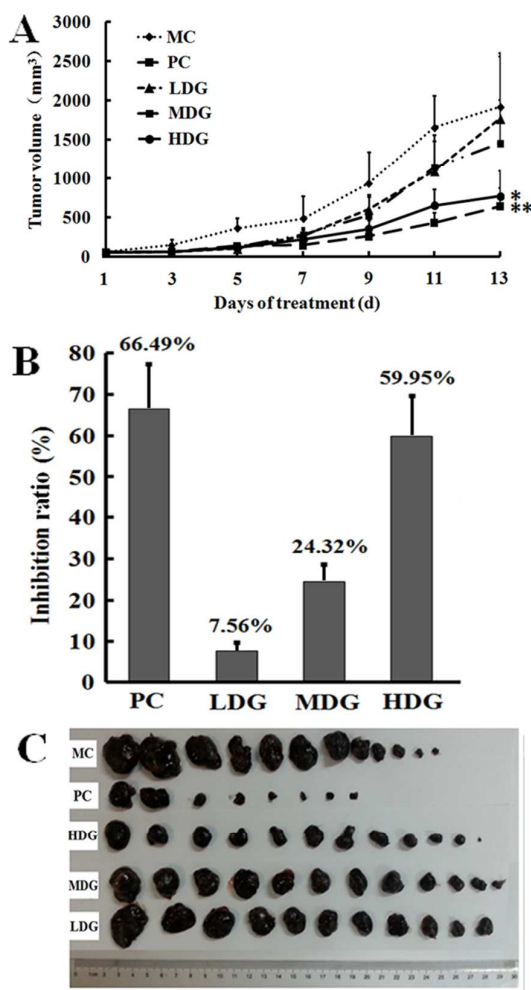
Figure 5. The antitumor effect of RPP against melanoma *in vivo*. A: therapeutic effects of RPP
and Docetaxel on the growth of B16F10 mouse melanoma tumor. Data was expressed as the mean
values ± S.E. (n=8). Differences were considered to be statistically significant when *$*P<0.05$*.
High significance was determined when *$**P<0.01$* compared to the model control. B: the tumor
volume inhibition ratio of each group. C: collected tumor tissue from each group.

3.5. RPP attenuates the reduced body weight of tumor-bearing mice

Figure 6 depicts the body weight of tumor-bearing mice before (white column)
and after (black column) treatment. The (final) net body weight has been calculated
according to the following equation: net body weight = body weight-tumor weight.
The initial weight of tumor-bearing mice in each group was similar before treatment.
However, along with the growth of tumor, the body weight loss of tumor-bearing mice
is significant, particularly in the model control group (▲$P<0.05$, ▲▲$P<0.05$ *vs.* initial
weight). Nevertheless, after RPP treatment, the reduced body weight of tumor-bearing

380   mice was found to be attenuated in a dose-dependent manner. Apparently, the high

381   dose of RPP inhibits the reduction in body weight of tumor-bearing mice compared

382   with the model control (**P<0.01*). Contrarily, the body weight of mice in the

383   positive control group shows no statistically significant difference compared to the

384   model control group.
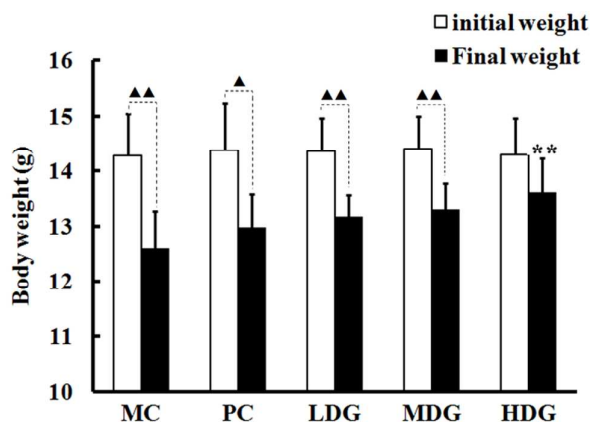
385

386   **Figure 6.** RPP suppressing the reduction in body weight of tumor-bearing mice. Data was
387   expressed as the mean values ± S.E. (n=8). Differences were considered to be statistically
388   significant when *P<0.05*. High significance was determined when *P<0.01*. Notes: **P<0.01 vs.*
389   model control; ▲*P<0.05,* ▲▲*P<0.01 vs.* initial weight.

390   *3.6. Immunostimulatory activity of RPP*

391   *3.6.1. Effect of RPP on the spleen index of tumor-bearing mice*

392   The spleen index of tumor-bearing mice has been calculated according to the

393   following equation: spleen index = spleen weight (g)/net body weight (kg). As it

394   shown in Figure 7, upon RPP administration, the spleen index of tumor-bearing mice

395   increases significantly and dose-dependently compared to the model control group

396   (**P<0.01*). In contrast, the spleen index of tumor-bearing mice in the positive

397   control group shows no statistically significant difference compared to the model

398   control group. Moreover, the spleen index-elevating effect of high dose RPP was

399   found to be considerably stronger compared to the positive control group ([#]*P<0.05*).

400   This result shows that RPP might exhibit an immunostimulatory effect.
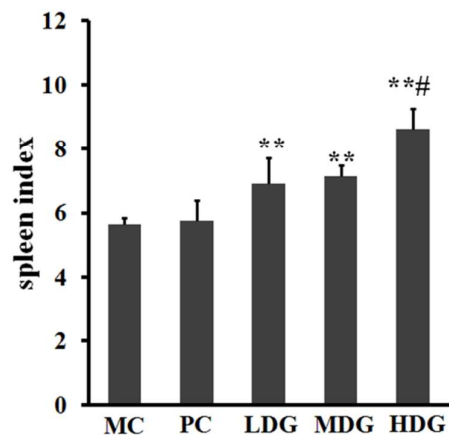
Figure 7. Effects of RPP on the spleen index of tumor-bearing mice. Data were expressed as the mean values ± S.E. (n=8). Differences were considered to be statistically significant when $P<0.05$. High significance was determined when $P<0.01$. Notes: **$P<0.01$ vs. model control; #$P<0.05$ vs. positive control.

3.6.2. RPP induces splenocyte proliferation in vitro

In order to confirm the immunostimulatory effect of RPP, a splenocyte proliferation assay has been carried out *in vitro*. As shown in Figure 8, in comparison with the blank control, conA significantly triggers splenocyte proliferation (**$P<0.01$). Similarly, the splenocytes in the RPP-treated groups increase in a dose-dependent manner (*$p<0.05$, **$P<0.01$ vs. blank control). However, Docetaxel was found to almost kill all splenocytes because of the strong cytotoxic effect of this agent (**$P<0.01$ vs. blank control). The data obtained indicate that RPP is able to induce the proliferation of splenocytes. The latter finding provides evidence for the hypothesis that RPP may demonstrate an immunostimulatory activity.
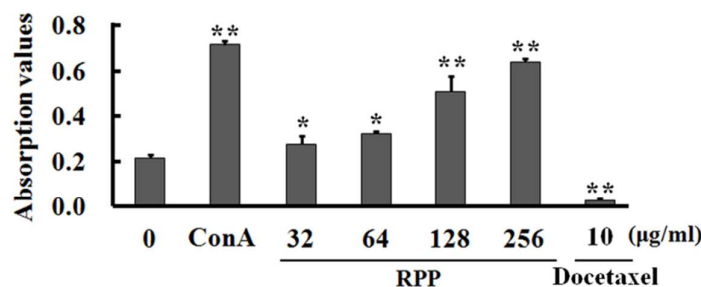
Figure 8. Effect of RPP on proliferation of splenocyte. Data were expressed as the mean values ± S.E. (n=5). Differences were considered to be statistically significant when *$p<0.05$. High significance was determined when **$P<0.01$ comparing with blank control.

3.6.3. RPP affects immune-related enzymes in the spleen of tumor-bearing mice

16

421   To investigate the mechanism of immunomodulation, we evaluated the effects of

422 RPP on several immune-related enzymes in the spleen of tumor-bearing mice. As

423 shown in Figure 9, RPP dose-dependently enhanced the activities of ACP (Figure 9A)

424 AKP (Figure 9B), LDH (Figure 9C) and SOD (Figure 9D) in the spleen of

425 tumor-bearing mice (*$P<0.05$, **$P<0.01$ vs. model control). In addition, the activities

426 of these enzymes in high dose of the RPP group was found to be significantly higher

427 than that in the positive control group ([#]$P<0.05$). While Docetaxel affects the

428 activities of ACP and SOD, it did not alter the activities of LDH and AKP (*$P<0.05$,

429 **$P<0.01$ vs. model control).
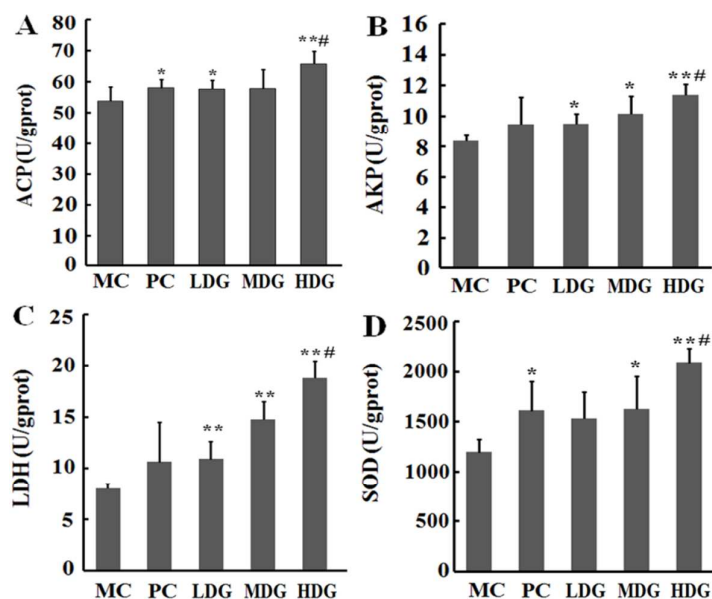
430

431 **Figure 9.** Effect of RPP on activities of acid phosphatase (ACP) (A), alkaline phosphatase (AKP)

432 (B), lactate dehydrogenase (LDH) (C) and superoxide dismutase (SOD) (D) in the spleen of

433 tumor-bearing mice. Data were expressed as the mean values ± S.E. (n=8). Differences were

434 considered to be statistically significant when $P<0.05$. High significance was determined when

435 $P<0.01$. Notes: *$P<0.05$, **$P<0.01$ vs. model control; [#]$P<0.05$ vs. positive control.

436 *3.6.4. RPP affects TNF-α, IFN-γ and IL-2 levels in the serum of tumor-bearing mice*

437   As shown in Figure 10, RPP dose-dependently increases serum concentrations of

438 TNF-α, IFN-γ and IL-2 (*$P<0.05$, **$P<0.01$ vs. model control). However, Docetaxel

439 had no obvious effect on IFN-γ, TNF-α and IL-2 in the serum of tumor-bearing mice.

440 Interestingly, the serum levels of these cytokines in medium and high dose of RPP

441 groups were significantly higher than the serum levels found in the positive control

442   group ($^{\#}P<0.05$, $^{\#\#}P<0.01$).

443
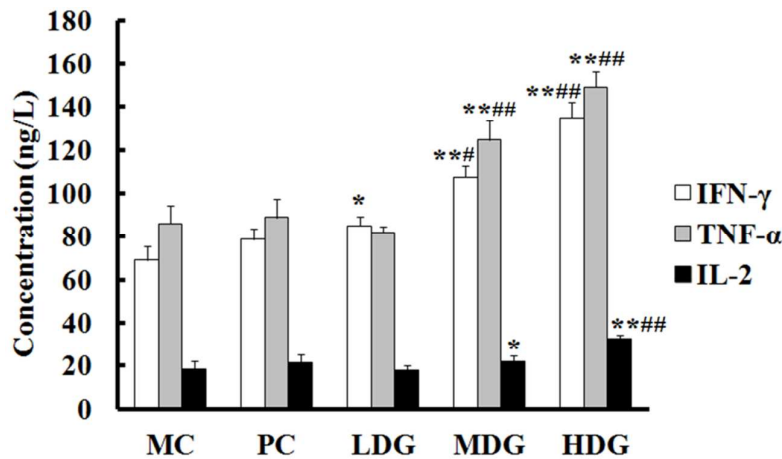
Figure 10. Effect of RPP on serum concentrations of interferon-γ (IFN-γ), interleukin 2 (IL-2) and tumor necrosis factor-α (TNF-α) in tumor-bearing mice. Data were expressed as the mean values ± S.E. (n=8). Differences were considered to be statistically significant when *P<0.05*. High significance was determined when *P<0.01*. Notes: *P<0.05, **P<0.01 *vs.* model control and $^{\#}P<0.05$, $^{\#\#}P<0.05$ *vs.* positive control.

3.7. Effects of RPP on histopathology of melanoma tissues

To further confirm the effect of RPP on melanoma, tumor tissues from C57BL/6 mice have been stained with hematoxylin and eosin (H&E) for histopathology analysis. As shown in Figure 11, tumor cells in the model control prove to be vital and show secretion of melanin (Figure 11-MC). However, the tumors in the Docetaxel-treated group display severe tissue necrosis. Docetaxel is known to target the nucleus of tumor cells and induce apoptosis (Figure 11-PC). RPP also induces necrosis of tumorous tissue, but unlike Docetaxel, inflammatory cells have been observed in the necrotic areas. Interestingly, the infiltration ratio of inflammatory cells increase with the dose of administered RPP (Figure 11-LDG, Figure 11-MDG and Figure 11-HDG).

460
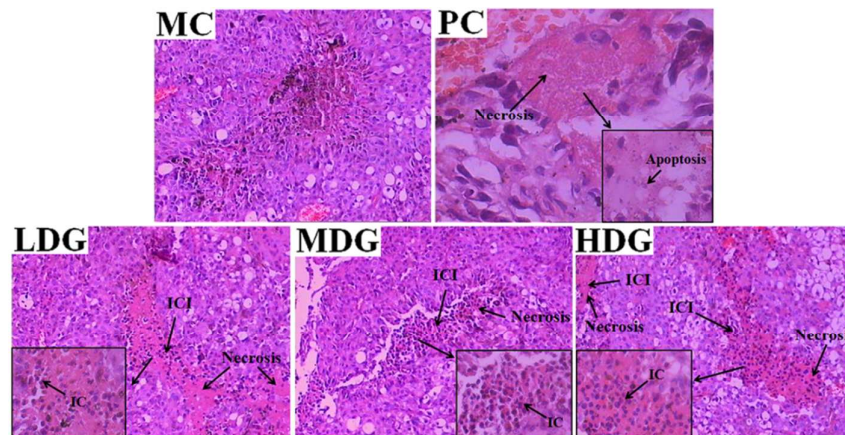
Figure 11. Effects of RPP on histopathology of melanoma tissue (H&E stain ×100 and ×400). ICI: inflammatory cell infiltration. IC: inflammatory cell.

3.8. Effects of RPP on histopathology of the liver and kidney

The changes in hepatic histology of different groups are shown in Figure 12. The hepatocytes in healthy mice exhibit an abundance of cytoplasm, distinct cell borders, round central nuclei and prove to be arranged in an ordered fashion (Figure 12-NC). However, the model group features necrosis of the hepatocytes in combination with infiltration of inflammatory cells (Figure 12-MC). Severe necrosis can also be observed in the Docetaxel-treated group due to the strong cytotoxic effect of Docetaxel (Figure 12-PC). In contrast, the hepatocytes in the RPP-treated groups show no obvious changes compared to healthy mice (Figure 12-LDG, Figure 12-MDG and Figure 12-HDG). This latter result indicates that RPP does indeed not induce liver lesions.
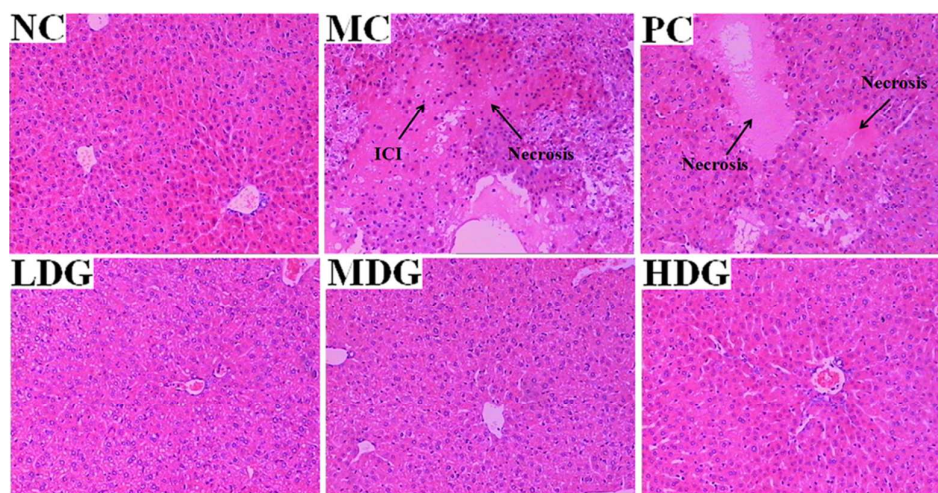
474

475 **Figure 12.** Effect of RPP on histopathology of the liver (H&E stain ×100). ICI: inflammatory cell

476 infiltrations.

477 As shown in Figure 13, the histopathology slices obtained from healthy mice

478 feature the integrated glomerulus with Bowman's capsule, renal cortex and an intact

479 glomerular basement membrane (Figure 13-NC). A few of glomerulus in the model

480 group show mesangial expansion compared to that of healthy mice (Figure 13-MC).

481 The glomerulus in the RPP-treated groups exhibits no obvious changes compared to

482 that of healthy mice (Figure 13-LDG, Figure 13-MDG and Figure 13-HDG). However,

483 in the Docetaxel-treated group, mesangial expansions can be observed (Figure 13-PC).

484 The results obtained suggest that RPP does not lead to any significant kidney

485 damages.
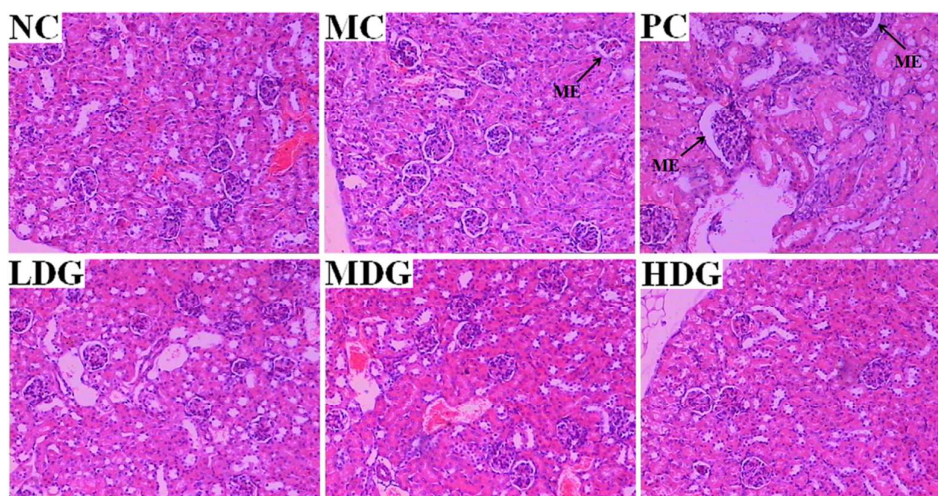
486

487 **Figure 13.** Effect of RPP on histopathology of the kidney (H&E stain ×100). ME: mesangial

488 expansion.

489 *3.9. Ability of RPP to enhance the chemotherapeutic effect of Docetaxel against*

490 *melanoma in vivo*

491 As shown in Figure 14-A, both Docetaxel and the combinatory RPP-Docetaxel

492 treatment significantly inhibit the growth of melanoma (***P<0.01 vs.* model control).

493 Surprisingly, the inhibitory effect of the combinatory RPP-Docetaxel treatment on

494 tumor growth is found to be significantly stronger than that of Docetaxel alone

495 (*#P<0.05*). The inhibition ratio of the tumor volume in the combinatory

496 RPP-Docetaxel group increases to 77.42%, approximately 12% higher than that for

497   the Docetaxel group (Figure 14-D). In addition, the combinatory RPP-Docetaxel

498   treatment reduces the body weight loss of tumor-bearing mice, an effect that has not

499   been observed in the group involving treatment with Docetaxel only (Figure 14-B).

500   Histopathology analyses of melanoma tissues from mice show that Docetaxel induces

501   a large area of tumor necrosis. Interestingly, upon combination with RPP, the

502   infiltration with inflammatory cells manifests in the necrotic areas (Figure 14-E). This

503   result suggests that the anti-melanoma effect of the chemotherapeutic drug Docetaxel

504   can be significantly improved upon combinatory administration of RPP *in vivo*.

505   Furthermore, the enhancement effect of RPP on the chemotherapeutic activity of

506   Docetaxel against malignant melanoma can most likely be ascribed to

507   immunopotentiation mechanisms.
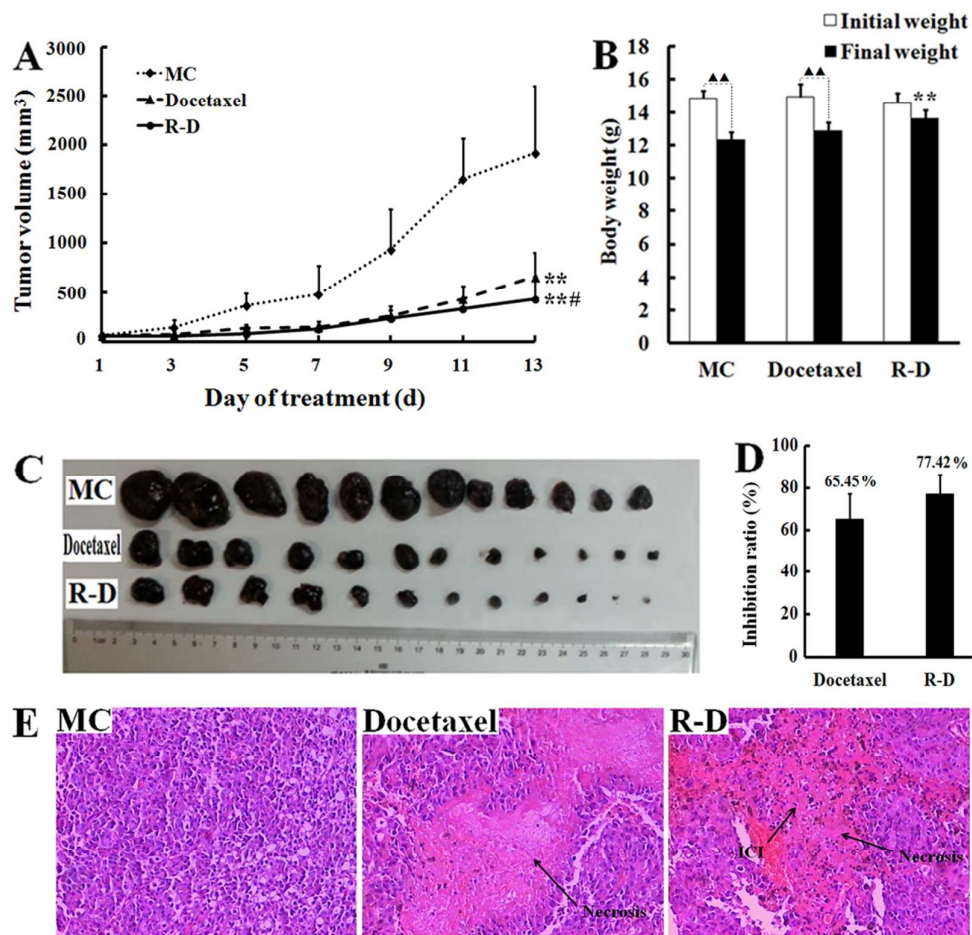
508
509   **Figure 14.** Ability of RPP to enhance the chemotherapeutic effect of Docetaxel against melanoma

510   *in vivo*. A: therapeutic effects of Docetaxel and combinatory RPP-Docetaxel on the growth of

511   B16F10 mouse melanoma. Data were expressed as the mean values ± S.E. (n=12). Differences

512   were considered to be statistically significant when *P<0.05*. High significance was determined

513   when *P<0.01*. Notes: ***P<0.01 vs.* model control, #*P<0.05 vs.* Docetaxel. B: body weight of each

514   group. Data were expressed as the mean values ± S.E. (n=12). Differences were considered to be

515   statistically significant when *P<0.05*. High significance was determined when *P<0.01*. Notes:

516   ***P<0.01 vs.* model control; ▲*P<0.05,* ▲▲*P<0.01 vs.* initial weight. C: collected tumor tissues

517   from each group. D: tumor volume inhibition ratio of each group. E: effect of Docetaxel and

518   combinatory RPP-Docetaxel treatment on histopathology of melanoma tissues (H&E stain ×100),

519   ICI: inflammatory cell infiltration.

520   *3.10. RPP alleviates liver and kidney injuries induced by Docetaxel*

521   As shown in Figure 15-A, the histopathology slices obtained from the model

522   indicate hepatocyte necrosis and inflammatory cell infiltration compared to the ones

523   obtained from healthy mice (Figure 15-A-NC and Figure 15-A-MC). Severe necrosis

524   can be observed in the Docetaxel-treated group as well (Figure 15-A-Docetaxel).

525   However, the hepatocyte necrotic area of the combinatory RPP-Docetaxel group is

526   found to be smaller than the necrotic tissue obtained from the group treated with

527   Docetaxel only. Moreover, the hepatocytes in the necrotic area are found to be not

528   extinct but degenerated (Figure 15-A-R-D).

529   As shown in Figure 15-B, a few of the glomeruli in the slices obtained from the

530   model group feature mesangial expansions compared to the slices obtained from

531   healthy mice (Figure 15-B-NC and Figure 15-B-MC). The group treated with

532   Docetaxel shows obvious mesangial expansions (Figure 15-B-Docetaxel). However,

533   the mesangial expansions almost completely disappear when Docetaxel was

534   combined with RPP and the structure of the glomerulus in the combinatory

535   RPP-Docetaxel treated group are similar to the normal control (Figure 15-B-R-D).

536   The results listed above provide evidence for the hypothesis that RPP can indeed

537   alleviate liver and kidney injuries induced by Docetaxel in tumor-bearing mice.
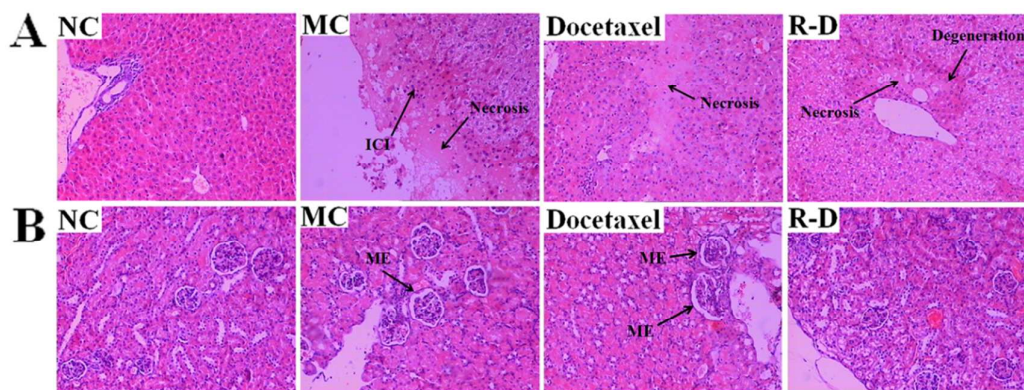
Figure 15. RPP alleviates liver (A) and kidney (B) injuries induced by Docetaxel (H&E stain ×100). ME: mesangial expansion; ICI: inflammatory cell infiltration.

4. Discussion

In recent decades, numerous polysaccharides exhibiting antitumor effects have been isolated from various plant sources. The individual antitumor mechanisms vary, depending on the polysaccharide species. Some polysaccharides show anti-proliferative effects against tumor cells, while others exhibit antitumor through improving the immune response of the host organism. For instance, polysaccharides from *Cordyceps militaris* inhibitthe proliferation of HT-29, Hela, HepG2 and K562 cells *in vitro* with half maximal inhibitory concentration (IC_{50}) values of 137.66, 162.59, 176.29 and 364.01 μg/ml, respectively [27]. *Portulaca oleracea* L. polysaccharides inhibit cervical carcinoma cell growth *in vitro* and *in vivo* [28]. Unlike the polysaccharides mentioned above, *Gynostemma pentaphyllum* polysaccharides show antitumor activity against hepatocellular carcinoma partly due to immunostimulation [10]. In the study presented here, RPP exhibits no obvious inhibitory effect on the proliferation of HT-29, MGC-803, Hela, Bel-7402, L02 and B16F10 cells *in vitro* (Figure 4). However, it exhibits high antitumor activity against malignant melanoma *in vivo* (Figure 5). In addition, compared to the chemical Docetaxel, RPP significantly reduces the body weight loss and causes no damage to the liver and kidney tissues in tumor-bearing mice (Figure 12 and Figure 13). The latter finding provides further evidence for the hypothesis that RPP exhibits no direct cytotoxic effect.

The spleen part of the secondary lymphoid tissue and splenocyte proliferation

562 plays a central role in the activation of both cellular and humoral immune responses

563 [29]. In the study presented here, RPP is believed to stimulate the proliferation of

564 splenocytes *in vitro* (Figure 8) which was found to be in agreement with the previous

565 *in vivo* study on the effect of RPP on spleen index of tumor-bearing mice (Figure 7).

566 The results obtained provide preliminarily evidence for RPP featuring potential

567 immunostimulatory effects.

568   Endogenous enzymes display crucial functions in the innate immune system, and

569 can serve as reliable markers in the assessment of the immune status [30].

570 Phagocytosis and encapsulation have been shown to represent the main elements of

571 insect cellular responses that play key roles against invading pathogens [31]. Here,

572 ACP and AKP are capable of assisting, modulating and accelerating phagocytosis [32].

573 Increased ACP and AKP activities have been demonstrated to accelerate the speed of

574 phagocytosis by modifying the surface molecular structures of pathogens [33]. SOD

575 plays important role as immune-related enzymes in enhancing the capability of

576 phagocytes and improving immune function [34]. The activity of LDH increases with

577 the activated macrophage and decreases with the inhibited macrophage [35]. In the

578 study presented here and in an effort to further investigate the immunostimulatory

579 mechanisms of RPP, the activities of ACP, AKP, SOD and LDH in the spleen of

580 tumor-bearing mice have been evaluated. The results obtained show that RPP is able

581 to significantly enhance the activities of ACP, AKP, LDH and SOD compared to the

582 model or Docetaxel-treated groups. This latter finding suggests that RPP is able to

583 increase cellular immune responses, including encapsulation and phagocytosis (Figure

584 9). However, recent studies have demonstrated that some chemotherapeutic agents

585 may exhibit immunomodulatory effects. Wang *et al.* found that human lung

586 adenocarcinoma cells display an increased sensitization towards lyses of CD3+

587 CD56+ cytokine induced killer (CIK) cells after treatment with nonlethal/sublethal

588 doses of Docetaxel *in vitro* [36]. Kroemer *et al.* reported that malignant cells can elicit

589 strong antitumor immune responses upon exposure to doxorubicin (Dox), which is

590 mediated by calreticulin (CRT) exposure and high-mobility group box 1 protein

591 (HMGB1) secretion on apoptotic cells [37]. In the present study, Docetaxel affects the

592   activity of ACP and SOD compared to the model group. The latter finding may be due

593   to the fact that Docetaxel inactivates melanoma cells by a direct cytotoxic effect and

594   further induces immune responses of the degenerating tumor cells to some extent.

595   Cytokines are a broad and loose category of small proteins participating in

596   intercellular signaling in both acquired and innate immunity. Among these biological

597   mediators, the role of TNF-α, IFN-γ and IL-2 is critical. IFN-γ is a critical cytokine

598   for innate and adaptive immunity and characterizes Th1 T cells, while IL-2 proves to

599   be a cytokine species associated with memory T cells, T cell proliferation and

600   differentiation. TNF-α is a pro-inflammatory cytokine that also serves as a neutrophil

601   chemoattractant [38]. In the present study, RPP significantly increases the serum

602   concentrations of TNF-α, IFN-γ and IL-2 in tumor-bearing mice, while the

603   chemotherapeutic agent Docetaxel alone exhibits no comparable effect (Figure 10).

604   Based on the results described above, we hypothesize that the inhibitory effect

605   exhibited by RPP on the growth of melanoma *in vivo* is most likely not due to the

606   direct cytotoxic effect on melanoma cells, but due to enhanced cellular immune

607   responses in tumor-bearing mice. These results suggest that RPP may find application

608   as a potential immunopotentiator in the treatment of malignant melanoma.

609   Despite recent progress on the development of more advanced chemotherapeutics,

610   no cure exists for some cancer types resulting in poor survival rates. Patients receiving

611   multiple cycles of chemotherapy are generally more prone to the development of

612   drug-resistance and a reduction in chemotherapeutic efficacy. Furthermore, increased

613   concentrations of chemotherapeutic drugs are typically associated with increased side

614   effects [39]. Combination therapy is frequently used in cancer treatment in an effort to

615   reduce drug resistance, alleviate adverse effects and enhance anticancer efficacy. In

616   recent years, multifaceted evidence has concentrated the scientific focus on some

617   biological macromolecules, including polysaccharides, to provide options to increase

618   the efficacy of conventional chemotherapy drugs. Zhang *et al.* reported that polyporus

619   polysaccharide displays synergistic effects and can effectively reduced the side effects

620   during Bacille Calmette-Guerin (BCG) instillation in rat bladder cancer models [40].

621   Furthermore, Zong *et al.* demonstrated that a sulfated polysaccharide, coined SIP-S

622 has the ability to significantly inhibit tumor growth in S180-bearing mice. Moreover,

623 combining SIP-S with cyclophosphamide (CTX) exhibited a higher anti-tumor

624 potency than CTX alone which may be associated with the immunostimulatory and

625 pro-apoptotic activities of SIP-S [41]. In the present study, we observed analogous

626 results. RPP can significantly enhance the antitumor effect of the chemotherapeutic

627 drug Docetaxel in melanoma-bearing mice, most likely due to immunopotentiation

628 (Figure 14). In addition, RPP is able to attenuate the side effects of Docetaxel therapy

629 *in vivo*, including the reduction of body weight loss in Docetaxel-treated

630 tumor-bearing mice. Furthermore, RPP has been shown to alleviate liver and kidney

631 damages caused by Docetaxel (Figure 15). This series of results indicate that RPP can

632 find potential application as a Docetaxel chemotherapeutic sensitizing and/or adjuvant

633 agent for the treatment of malignant melanoma.

634 5. Conclusions

635   In summary, this study demonstrates the *in vivo* antitumor activity of raspberry

636 pulp polysaccharide (RPP) against melanoma. The inhibitory effect of RPP on the

637 growth of melanoma is not found to be due to direct cytotoxic effects. However, the

638 effects observed are most likely due to immunipotentiating effects, i.e. enhancements

639 of the immune system in tumor-bearing mice. Furthermore, RPP enhances the

640 therapeutic effect of Docetaxel against malignant melanoma *in vivo* and alleviates the

641 Docetaxel-induced liver and kidney lesions in tumor-bearing mice. Another crucial

642 feature presented in this study shows that RPP is non-toxic and can therefore

643 potentially be used as an immunopotentiator and/or as an adjuvant chemotherapeutic

644 agent for the future treatment of malignant melanoma. To further substantial this latter

645 notion, more studies have to be performed prior to justifying any clinical trials.

646 Conflict of interest

647   The authors declare no conflicts of interest.

648 Ackonwledgments

651

652   **References**

653   [1] P. Shao, X. X. Chen and P. L. Sun, *In vitro* antioxidant and antitumor activities of different

654   sulfated polysaccharides isolated from three algae. *Int. J. Biol. Macromol.*, 2013, 62, 155-161.

655   [2] Y. Kato, I. Yoshino, R. Pili, C. Egusa, T. Maeda and R. Tsuboi, Combination of HDAC

656   inhibitor MS-275 and IL-2 increased anti-tumor effect in a melanoma model via activated

657   cytotoxic T cells, *J. Dermatol. Sci.*, 2014, 75, 140-147.

658   [3] T. T. Sreelekha, S. Varghese, M. M. Joseph, S. K. George and S. R. Aravind, A galactomannan

659   polysaccharide from *Punica granatum* imparts *in vitro* and *in vivo* anticancer activity, *Carbohyd.*

660   *Polym.*, 2013, 98, 1466-1475.

661   [4] C. Y. Wang, Y. Wang, J. Zhang, Z. Y. Wang, Optimization for the extraction of

662   polysaccharides from *Gentiana scabra* Bunge and their antioxidant *in vitro* and anti-tumor activity

663   *in vivo*, *J. Taiwan Inst. Chem. E.*, 2014, 45, 1126-1132.

664   [5] C. X. Jiang, L. Zhao, S. L. Li, X. R. Zhao, Q. H. Zhang and Q. P. Xiong, Preliminary

665   characterization and immunostimulatory activity of polysaccharides from *Glossaulax didyma*,

666   *Food Chem. Toxicol.*, 2013, 62, 226-230.

667   [6] H. L. Zhang, J. Li, J. M. Xia and S. Q. Lin, Antioxidant activity and physicochemical

668   properties of an acidic polysaccharide from *Morinda officinalis*, *Int. J. Biol. Macromol.*, 2013, 58,

669   7-12.

670   [7] Z. G. Qian, Cellulase-assisted extraction of polysaccharides from *Gucurbita moschata* and

671   their abtibacterial activity, *Carbohyd. Polym.*, 2014, 101, 432-434.

672   [8] C. Guo, R. Li, N. Zheng, L. Y. Xu, T. Liang and Q. L. He, Anti-diabetic effect of ramulus mori

673   polysaccharides, isolated from *Morus alba* L., on STZ-diabetic mice through blocking

674   inflammatory response and attenuating oxidative stress, *Int. Immunopharmacol.*, 2013, 16, 93-99.

675   [9] E. Beat and M. John L, From carbohydrate leads to glycomimetic drugs, *Nat. Rev. Drug*

676   *Discov.*, 2009, 8, 661-677.

677   [10] J. Liu, L. H. Zhang, Y. G. Ren, Y. L. Gao, L. Kang, Q. Qiao, Anticancer and

678   immunoregulatory activity of *Gynostemma pentaphyllum* polysaccharides in H22 tumor-bearing

679   mice, *Int. J. Biol. Macromol.*, 2014, 69, 1-4.

680   [11] G. W. Shu, W. H. Zhao, L. Yue, H. W. Su, M. X. Xiang, Antitumor immunostimulatory

681   activity of polysaccharides from *Salvia chinensis* Benth, *J. Ethnopharmacol.*, 2015, 168, 237-247.

682   [12] C. S. Bowen-Forbes, Y. J. Zhang, M. G. Nair, Anthocyanin content, antioxidant,

683   anti-inflammatory and anticancer properties of blackberry and raspberry fruits, *J. Food Compos.*

684   *Analy.*, 2010, 23, 554-560.

685   [13] A. Crozier, G. G. Duthie, P. Gardner, M. E. J. Lean, M. R. MacLean, J. McGinn, W. Mullen,

686   T. Yokota, Ellagitannins, flavonoids, and other phenolics in red raspberries and their contribution

687   to antioxidant capacity and vasorelaxation properties, *J. Agr. Food Chem.*, 2002, 50, 5191-5196.

688   [14] M. A. Poiana, D. Moigradean, D. Raba, L. M. Alda, M. Popa, The effect of long-term frozen

689   storage on the nutraceutical compounds, antioxidant properties and color indices of different kinds

690 of berries, *J. Food Agric. Environ.*, 2010, 8, 54-58.

691 [15] M. Kubota, C. Ishikawa, Y. Sugiyama, S. Fukumoto, T. Miyagi, S. Kumazawa, Anthocyanins

692 from the fruits of *Rubus croceacanthus* and *Rubus sieboldii*, wild berry plants from Okinawa,

693 Japan, *J. Food Compos. Analy.*, 2012, 28, 179-182.

694 [16] S. A. M. Hussein, N. A. Ayoub, M. A. M. Nawwar, Caffeoyl sugar esters and an ellagitannin

695 from *Rubus sanctus*, *Phytochemistry*, 2003, 63, 905-911.

696 [17] W. Mullen, M. E. J. Lean, A. Crozier, Rapid characterization of anthocyanins in red

697 raspberry fruit by high-performance liquid chromatography coupled to single quadrupole mass

698 spectrometry, *J. Chromatogr. A*, 2002, 966, 63-70.

699 [18] X. X. Chen, S. D. Zhou, Y. W. Ou, S. Y. Xiao, W. H. Lin, Y. Cao, M. Zhang, L. C. Zhao, L.

700 F. Li, Additional ent-Kaurane Diterpenoids from *Rubus corchorifolius* L. f, *Helv. Chim. Acta*,

701 2010, 93, 84-89.

702 [19] S. E. Im, T. G. Nam, H. Lee, M. W. Han, H. J. Heo, S. I. Koo, C. Y. Lee, D. O. Kim,

703 Anthocyanins in the ripe fruits of *Rubus coreanus Miquel* and their protective effect on neuronal

704 PC-12 cells, *Food Chem.*, 2013, 139, 604-610.

705 [20] T. P. Lien, C. Kamperdick, T. V. Sung, G. Adam, Triterpenes from *Rubus cochinchinensis*,

706 *Phytochemistry*, 1999, 50, 463-465.

707 [21] H. X. Kuang, Y. G. Xia, J. Liang, B. Y. Yang, Q. H. Wang and Y. P. Sun, Fast classification

708 and compositional analysis of polysaccharides from TCMs by ultra-performance liquid

709 chromatography coupled with multivariate analysis, *Carbohyd. Polym.*, 2011, 84, 1258-1266.

710 [22] L. Y. Zhao, Y. H. Dong, G. T. Chen and Q. H. Hu, Extraction, purification, characterization

711 and antitumor activity of polysaccharides from Ganoderma lucidum, *Carbohyd. Polym.*, 2010, 80,

712 783-789.

713 [23] W. H. Ni, T. T. Gao, H. L. Wang, Y. Z. Du, J. Y. Li, L. X. Wei and H. T. Bi, Anti-fatigue

714 activity of polysaccharides from the fruits of four Tibetan plateau indigenous medicinal plants, *J.*

715 *Ethnopharmacol.*, 2013, 150, 529-535.

716 [24] X. Y. Li, Z. Y. Wang and L. Wang, Polysaccharide of *Hohenbuehelia serotina* as a defense

717 against damage by whole-body gamma irradiation of mice, *Carbohyd. Polym.*, 2013, 94, 829-835.

718 [25] X. J. Jia, L. H. Dong, Y. Yang, S. Yuan, Z. W. Zhang and M.Yuan, Preliminary structural

719 characterization and antioxidant activities of polysaccharides extracted from Hawk tea (Litsea

720 coreana var.lanuginosa), *Carbohyd. Polym.*, 2013, 95, 195-199.

721 [26] Z. F. Zhang, G. Y. Lv, W. Q. He, L. G. Shi, H. J. Pan and L. F. Fan, Effects of extraction

722 methods on the antioxidant activities of polysaccharides obtained from *Flammulina velutipes*,

723 *Carbohyd. Polym.*, 2013, 98, 1524-1531.

724 [27] Y. S. Jing, X. L. Cui, Z. Y. Chen, L. J. Huang, L. Y. Song, T. Liu, Elucidation and biological

725 activities of a new polysaccharide from cultured *Cordydeps militaris*, *Carbohyd. Polym.*, 2014,

726 102, 288-296.

727 [28] R. Zhao, X. Gao, Y. P. Cai, X. Y. Shao, G. Y. Jia, Y. L. Huang, X. G. Qin, J. W. Wang, X. L.

728   Zheng, Antitumor activity of *Portulaca oleracea* L. polysaccharides against cervical carcinoma *in*

729   *vitro* and *in vivo*, *Carbohyd. Polym.*, 2013, 96, 376-383.

730   [29] J. T. Wei, S. X. Wang, G. Liu, D. Pei, Y. F. Liu, Y. Liu and D. L. Di, Polysaccharides from

731   Enteromorpha prolifera enhance the immunity of normal mice, *Int. J. Biol. Macromol.*, 2014, 64,

732   1-5.

733   [30] Y. Xia, P. Dean, A. J. Judge, J. P. Gillespie, J. M. Clarkson, A.K. Charnley, Acid

734   phosphatases in the haemolymph of the desert locust, Schistocerca gregaria, infected with the

735   entomopathogenic fungus Metarhizium anisopliae, *J. Insect Physiol.*, 2000, 46, 1249-1257.

736   [31] M. W. Lingen, Role of Leukocytes and Endothelial Cells in the Development of Angiogenesis

737   in Inflammation and Wound Healing, *Arch. Pathol. Lab. Med.*, 2001, 125, 67-71.

738   [32] G. Q. Wu, Y. H. Yi, Effects of dietary heavy metals on the immune and antioxidant systems

739   of *Galleria mellonella* larvae, *Comp. Biochem. Phys. C*, 2015, 167, 131-139.

740   [33] G. Q. Wu, Y. H. Yi, Y. Y. Lv, M. Li, J. Wang, L. H. Qiu, The lipopolysaccharide (LPS) of

741   Photorhabdus luminescens TT01 can elicit dose- and time-dependent immune priming in Galleria

742   mellonella larvae, *J. Invertebr. Pathol.*, 2015,127, 63-72.

743   [34] J. Du, H. X. Zhu, P. Liu, J. Chen, Y. J. Xiu, W. Yao, T. Wu, Q. Ren, Q. G. Meng, W. Gu and

744   W. Wang, Immune responses and gene expression in hepatopancreas from *Macrobrachium*

745   *rosenbergii* challenged by a novel pathogen spiroplasma MR-1008, *Fish Shellfish Immu.*, 2013, 34,

746   315-323.

747   [35] X. M. Chen, J. X. Lu, Y. D. Zhang, J. T. He, X. Z. Guo, G. Y. Tian and L. Q. Jin, Studies of

748   macrophage immune-modulating activity of polysaccharides isolated from Paecilomyces tenuipes,

749   *Int. J. Biol. Macromol.*, 2008, 43, 252-256.

750   [36] W. J. Wang, S. H. Qin, L. Zhao, Docetaxel enhances CD3+ CD56+ cytokine-induced killer

751   cells-mediated killing through inducing tumor cells phenotype modulation, *Biomed.*

752   *Pharmacother.*, 2015, 69, 18-23.

753   [37] L. Zitvogel, O. Kepp, L. Senovilla, L. Menger, N. Chaput, G. Kroemer, Immunogenic tumor

754   cell death for optimal anticancer therapy: the calreticulin exposure pathway, *Clin. Cancer. Res.*,

755   2010, 16, 3100-3104.

756   [38] I. Leroux-Roels, J. M. Devaster, G. Leroux-Roels, V. Verlant, I. Henckaerts, P. Moris, P.

757   Hermand, P. V. Belle, J. T. Poolman, P. Vandepapeliere and Y. Horsmans, Adjuvant system

758   AS02Venhances humoral and cellular immuneresponses to pneumococcal protein PhtD vaccine in

759   healthy youngand older adults: Randomised, controlled trials, *Vaccine*, 2015, 33(4), 577-584.

760   [39] M. Sun, W. Y. Zhao, Q. P. Xie, Y. H. Zhan and B. Wu, Lentinan reduces tumor progression

761   by enhancing gemcitabine chemotherapy in urothelial bladder cancer, *Surg. Oncol.*, 2014,

762   DOI:10.1016/j.suronc.2014.11.002.

763   [40] G. W. Zhang, G. F. Qin, B. Han, C. X. Li, H. G. Yang, P. H. Nie, X. Zeng, Efficacy of

764   Zhuling polyporus polysaccharide with BCG to inhibit bladder carcinoma, *Carbohyd. Polym.*,

765   2015, 118, 30-35.

766   [41] A. Z. Zong, Y. H. Liu, Y. Zhang, X. L. Song, Y. K. Shi, H. Z. Cao, C. H. Liu, Y. N. Cheng, W.

767   J. Jiang, F. L. Du, F. S. Wang, Anti-tumor activity and the mechanism of SIP-S: A sulfated

768   polysaccharide with anti-metastatic effect, *Carbohyd. Polym.*, 2015, 129, 50-54.

Raspberry pulp polysaccharide exhibits antitumor activity *in vivo* against malignant melanoma through immunipotentiation and enhances the antitumor effect of Docetaxel.